Semiconductor-Nanowire-Based Superconducting Qubit

First report

Advisor：Professor Kuei-Lin Chiu
Reporter：Yung-Xiang Chen

2020/09/22

Outline

- Principle of qubit
- Gatemon
- Property of gatemon
- Fig.2
  - Spectrum of gatemon
  - Coupling energy of gatemon
- Fig.3
  - “Vg-Qubit drive” diagram
  - Rabi oscillation
  - Z-rotation
- Fig.4
  - T1 & T2 measurement
  - Coherence time of gatemon
  - Hahn echo experiment
- Improvement

Qubit principle

- A form of LC oscillator.
- The inductor part is Josephson Junciton, a non-linear inductor.
- $I = I_C \sin \varphi$
- observe commute law
- correspondibg eigenenergy of system：

$$E_{\pm,n} = -\frac{1}{2}\hbar\omega_A + (n+1)\hbar\omega_C \pm 12\hbar\Omega_n$$

where $\Omega_n = \sqrt{4g^2(n+1) + \Delta^2}$

$$\Delta = \omega_A - \omega_C$$

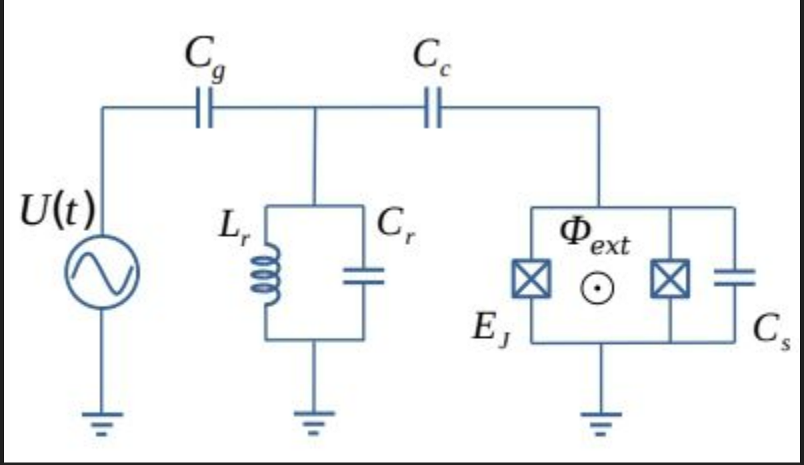

Gatemon

- SNS JJ's
- InAs at midle and Al is aside
- The total capacitance C is determined by T-shape Al island and surrounding Al ground plane
- The cavity is used for dispersive readout
- Cavity and qubit are patterned by wet etching Al film on an oxidised high resistively Si substrate

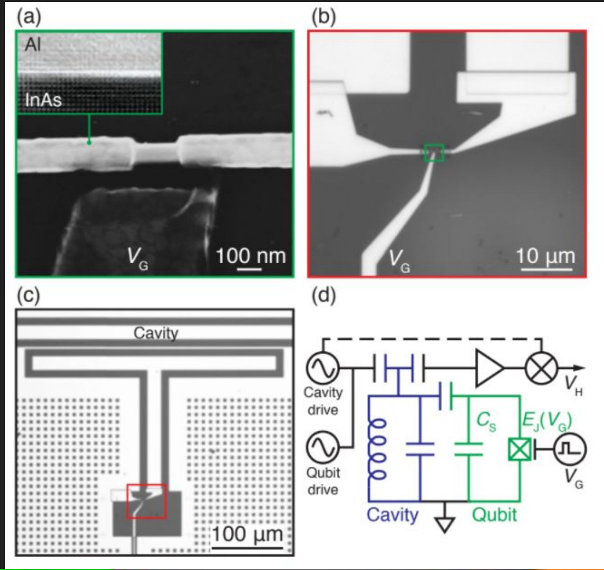

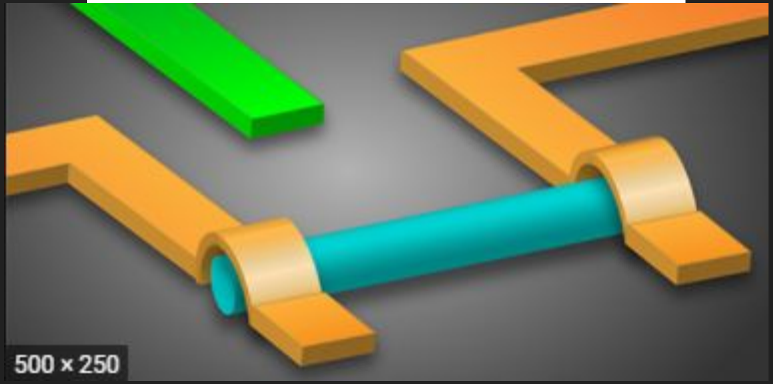

Property of gatemon

- Schotty-barrier free SN interference
- The electron density of semiconductor core is controlled by electric gate, V_G
- The transition frequency is given by $f_Q = E_{01}/h = \sqrt{8E_J E_c}/h$
- Gatemon operate with $E_j \gg E_C$

  where charge energy $E_C = e^2/2C_\Sigma$

Fig.2,(a)&(b)

~ Spectrum of gatemon

- The diagram shows that the function of V_G has a periodical fluctuation between the transition peaks.
- The periodical fluctuation has related to endoscopic fluctuation, which also can be found in normal-state conductor.
- This results $f_Q \propto \sqrt{I_c(V_G)}$
- We can see as f_Q increasing, the f_c corresponding.

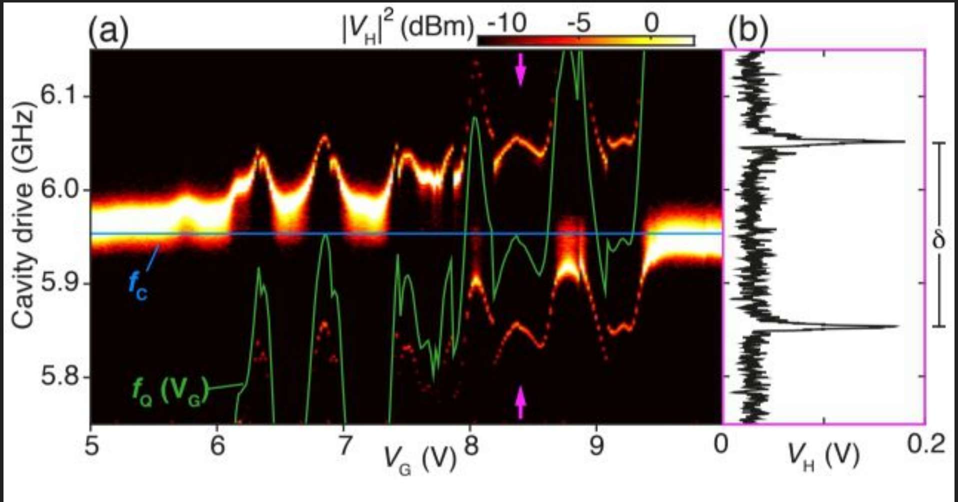

- The separate peaks indicate the strong coupling regime between the qubit and cavity.

Fig.2,(c)&(d)

~ Coupleing energy of gatemon

- The coupling strength allow Rabi splitting to be resolved, writing the hybrid qubit-cavity state frequency as

$$\lambda_{\pm} = \left(f_Q + f_c \pm \sqrt{\left(f_Q - f_c\right)^2 + 4(g/2\pi)^2} \right) /2$$

- The qubit-cavity coupling strength, $g/2\pi$, is extracted from fitting the solid theory curve.
- We also can observe two lines avoid to engage.

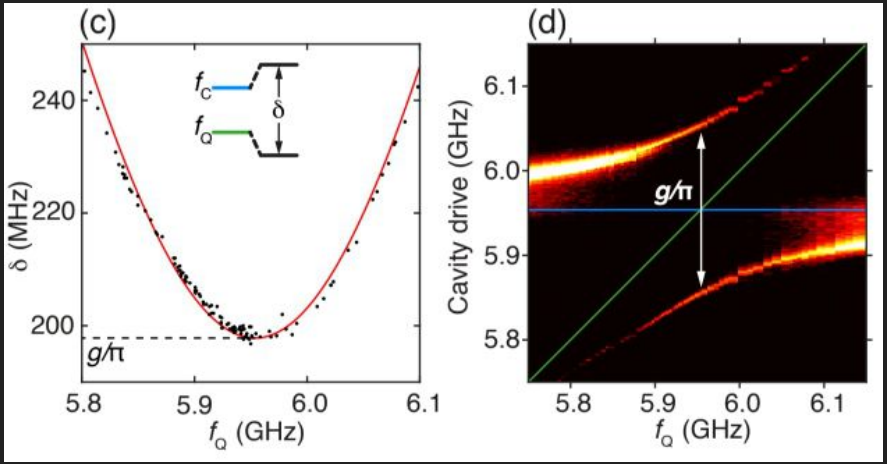

Fig.3,(a)

~ “Vg-Qubit drive” diagram

- When qubit drive was on resonance with f_Q , a peak in the cavity response was observed, yielding a reproducible gate voltage dependence.
- fig3b is measured by changing the qubit drive frequency and pluse time.
- which can also observe the Rabi oscillation.
- Those dynamic control is important for fast two qubit operator, especially when two qubit are coupling to each other.
- fig3c show operation of the Z-rotation
  a. use $R_X^{\pi/2}$ gate to rotate to $\frac{1}{\sqrt{2}}(|0> + |1>)$ (~15us)
  b. excute the V_G pulse(time τ, amplitude ΔV_G)
  c. excute $R_X^{\pi/2}$ gate to rotate around x-axis(~15us)
  d. observe the probability density

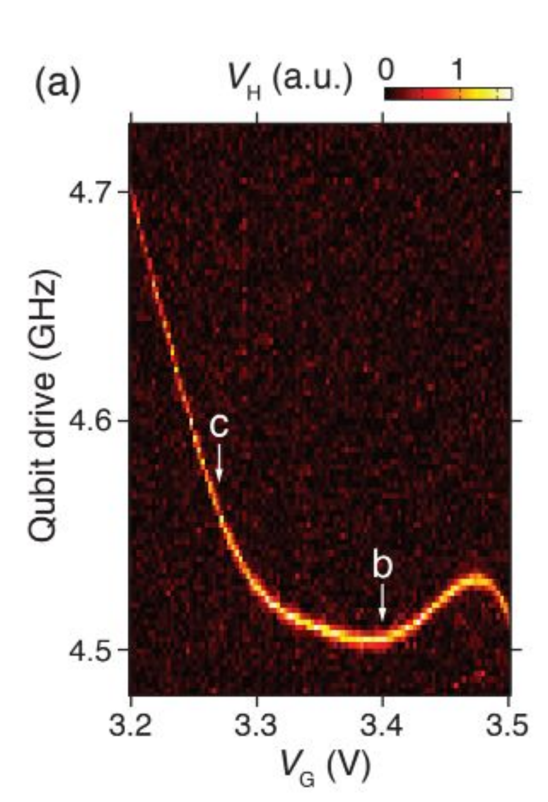

Fig.3,(b)

~ Rabi oscillation

- When qubit drive was on resonance with f_Q , a peak in the cavity response was observed, yielding a reproducible gate voltage dependence.
- fig3b is measured by changing the qubit drive frequency and pluse time.
- which can also observe the Rabi oscillation.
- Those dynamic control is important for fast two qubit operator, especially when two qubit are coupling to each other.
- fig3c show operation of the Z-rotation
    a. use $R_X^{\pi/2}$ gate to rotate to $\frac{1}{\sqrt{2}}(|0> + |1>)$ (∼15us)
    b. excute the V_G pulse(time τ, amplitude ΔV_G)
    c. excute $R_X^{\pi/2}$ gate to rotate around x-axis(∼15us)
    d. observe the probability density

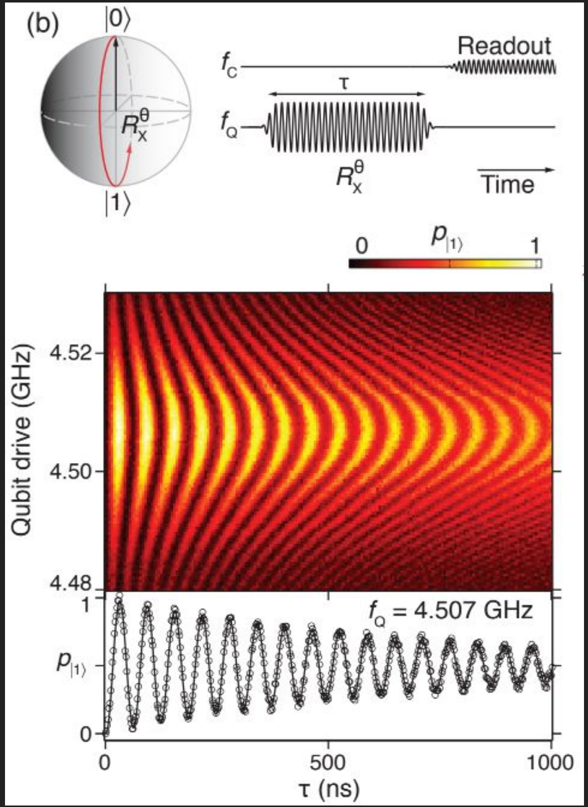

Fig.3,(b)

~ Z-rotation

- When qubit drive was on resonance with f_Q , a peak in the cavity response was observed, yielding a reproducible gate voltage dependence.
- fig3b is measured by changing the qubit drive frequency and pluse time.
- which can also observe the Rabi oscillation.
- Those dynamic control is important for fast two qubit operator, especially when two qubit are coupling to each other.
- fig3c show operation of the Z-rotation
    a. use $R_X^{\pi/2}$ gate to rotate to $\frac{1}{\sqrt{2}}(|0> + |1>)$ (~15us)
    b. excute the V_G pulse(time τ, amplitude ΔV_G)
    c. excute $R_X^{\pi/2}$ gate to rotate around x-axis(~15us)
    d. observe the probability density

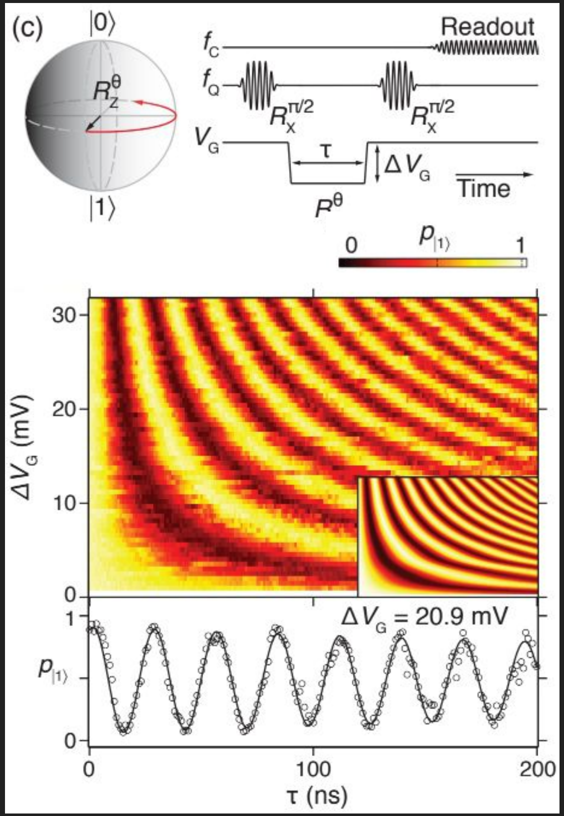

Fig.4

~ T1 & T2 measurement

- T1 measurement:
  a. Let qubit be excited to I1> ($R_X^{\pi/2}$ ~30ns)
  b. waiting for varying time τ
  c. measure
  d. eistimate by equation:
     - $S(t) = S(0)\exp(t/T_1)$
- T2 measurement ~ Ramsey measurement
- Extra experiment: Hahn echo experiment

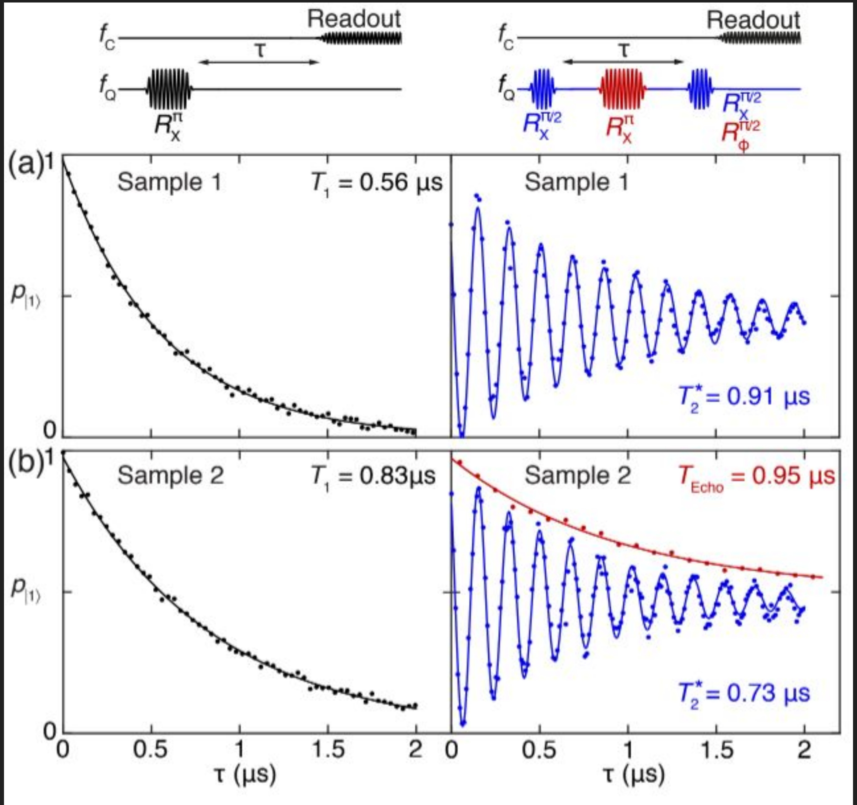

Fig.4,

～coherence time of gatemon

- Sample1(at b point, V_G =3.4V)：
    - T_1 =0.56us
    - T_2^* =0.91us
- $T_2^* = 2T_1$
- The team think that the coherence was limited by energy relaxation time at this operating point
- Sample2(at c point, Vg=-11.3)
    - T_1 =0.83us(relative longer)
    - T_2^* =0.73us(relative shorter)

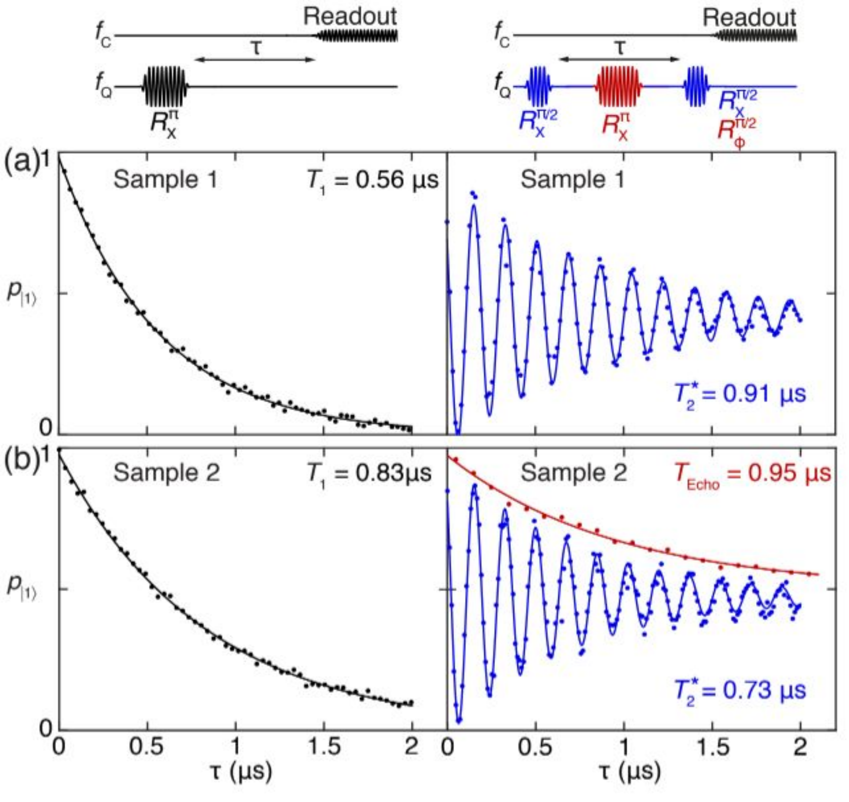

Fig.4,

～Hahn echo experiment

- Hahn echo experiment～applying Hahn echo pulse sequence effectively reduced low frequency noise in f_Q
- increase the dephasing time to T_{echo}=0.95us, implied second device has great degree of low frequency noise in Ej(Vg)
- Techo doesn’t reach $2T_1$ indicate that higher frequency noise fluctuation faster than t also contribute to dephasing

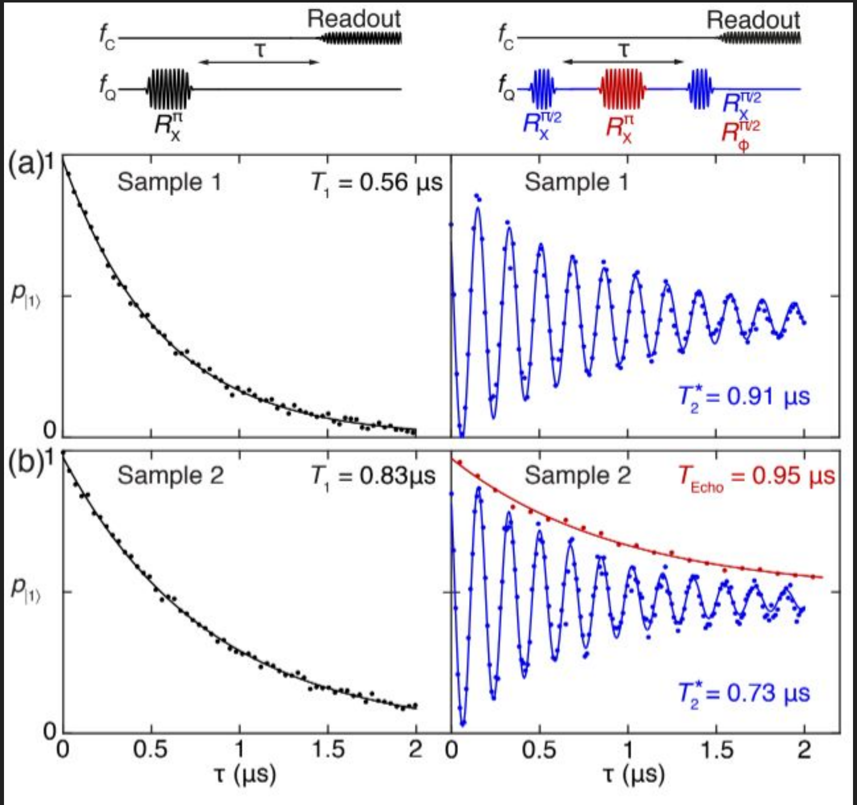

improvement

- removing the SiO_2 dielectric layer
- better sample processing
- reduce the interface loss in the capacitor
- increase maganetic and infrared radiation shielding

The end